Published in final edited form as:
Circulation. 2009 March 17; 119(10): 1386–1397. doi:10.1161/CIRCULATIONAHA.108.802918.

DIVERGENT TNF RECEPTOR-RELATED REMODELING RESPONSES IN HEART FAILURE: Role of NF-κB and Inflammatory Activation

Tariq Hamid, PhD, **Yan Gu, MD, PhD**, **Roger V. Ortines, BS**, **Chhandashri Bhattacharya, MS**, **Guangwu Wang, MD, PhD**, **Yu-Ting Xuan, PhD**, and **Sumanth D. Prabhu, MD**
Institute of Molecular Cardiology, Department of Medicine, University of Louisville and Louisville VAMC, Louisville, KY

Abstract

Background—Although pre-clinical data suggested that tumor necrosis factor-α (TNF) neutralization in heart failure (HF) would be beneficial, clinical trials of TNF antagonists were paradoxically negative. We hypothesized that TNF induces opposing inflammatory and remodeling responses in HF that are TNF-receptor (TNFR) specific.

Methods and Results—HF was induced in wild-type (WT), TNFR1−/−, and TNFR2−/− mice via coronary ligation. Compared to WT HF, 4-week post-infarction survival was significantly improved in both TNFR1−/− and TNFR2−/− HF. Compared to sham, WT HF hearts exhibited significant remodeling with robust activation of nuclear factor(NF)-κB, p38 MAPK, and JNK2, and upregulation of TNF, interleukin(IL)-1β, IL-6, and IL-10. Compared to WT HF, TNFR1−/− HF exhibited: 1) improved remodeling, hypertrophy, and contractile function; 2) less apoptosis; and 3) diminished NF-κB, p38 MAPK, and JNK2 activation and cytokine expression. In contrast, TNFR2 −/− HF had exaggerated remodeling and hypertrophy, increased border zone fibrosis, augmented NF-κB and p38 MAPK activation, higher IL-1β and IL-6 gene expression, greater activated macrophages, and greater apoptosis. Oxidative stress and diastolic function were improved in both TNFR1−/− and TNFR2−/− HF. In H9c2 cardiomyocytes, sustained NF-κB activation was pro-apoptotic, an effect dependent on TNFR1 signaling, whereas TNFR2 overexpression attenuated TNF-induced NF-κB activation.

Conclusions—TNFR1 and TNFR2 have disparate and opposing effects on remodeling, hypertrophy, NF-κB and inflammation, and apoptosis in HF: TNFR1 exacerbates, whereas TNFR2 ameliorates, these events. However, signaling through both receptors is required to induce diastolic dysfunction and oxidative stress. TNF receptor-specific effects in HF should be considered when developing therapeutic anti-TNF strategies.

Keywords

TNF; TNF receptor; heart failure; cardiac remodeling; NF-κB; inflammation

Circulating levels of tumor necrosis factor-α (TNF) and soluble TNF receptors (TNFRs) are independent predictors of mortality in patients with heart failure (HF) [1]. TNF antagonism is cardioprotective in rats subjected to continuous TNF infusion [2], in mice with cardiac-

Correspondence: Sumanth D. Prabhu, MD, Medicine/Cardiovascular Medicine, University of Louisville, ACB, 3rd Floor, 550 South Jackson Street, Louisville, KY 40202, Telephone: (502) 852-7959, Fax: (502) 852-7147, sprabhu@louisville.edu.

CONFLICT OF INTEREST DISCLOSURES
There are no commercial affiliations or conflicts of interest to disclose.

restricted TNF overexpression [3], and in experimental animal models of HF [4,5]. These and other studies suggested that TNF blockade in HF would result in clinical improvement. Surprisingly, however, randomized trials of anti-TNF therapy in human HF failed to show benefit, and unexpectedly demonstrated a time- and dose-related increase in death and HF hospitalization [1]. Hence, whether or not TNF is a viable therapeutic target in HF remains largely unresolved.

The paradoxical clinical trial results implied a more complicated role for TNF in HF than is currently considered. Indeed, TNF-mediated effects are not uniformly detrimental in the heart. As a stress-response protein, TNF is cytoprotective during conditions such as ischemic injury [6], coronary microembolization [7], and infectious myocarditis [8]. TNF signaling occurs via two cell-surface receptors (TNFR1 and TNFR2), and in large part via the TRAF2 (TNFR-associated factor 2)-dependent activation of nuclear factor (NF)-κB, p38 mitogen activated protein kinase (MAPK), and c-Jun N-terminal kinase (JNK) [9]. We tested the hypothesis that TNF induces dichotomous effects in HF based on the relative contribution of TNFR1- and TNFR2-dependent inflammatory signaling *in vivo*. Our results establish that TNFR-specific effects in HF relate to both pathological remodeling and NF-κB activation, such that TNFR1 induces persistent NF-κB activation and accelerates remodeling, whereas TNFR2 counterbalances these effects. Moreover, these unique and divergent inflammatory responses specific to each TNF receptor in the failing heart suggest that global TNF inhibition, as was done in clinical trials, would abrogate both protective as well as detrimental effects.

METHODS

Please see the expanded Methods in the online supplement. All studies were performed in compliance with the NIH Guide for the Care and Use of Laboratory Animals (DHHS publication [NIH] 85-23, revised 1996). The authors had full access to and take full responsibility for the integrity of the data. All authors have read and agree to the manuscript as written.

Mouse models

Male mice 12–28 weeks of age were used. TNFR1−/− and TNFR2−/− mice were obtained from Jackson Laboratories (Stock #002818 and #002620, respectively). The background strain, C57BL/6 (#000664), was used as wild-type (WT) control.

Coronary ligation and experimental protocol

After the induction of anesthesia with tribromoethanol (0.25 mg/g IP), mice were intubated and supported with a MiniVent Mouse Ventilator (Harvard Apparatus) and anesthesia was maintained with 1% isoflurane. Under sterile conditions, the heart was exposed via a left thoracotomy in the 4^{th} intercostal space. An 8.0 prolene ligature was passed and tied around the proximal left coronary artery (HF group). In sham animals, the suture was passed but not tied. The chest was then closed using 5.0 silk. The total mice used were: C57BL/6 n = 90; TNFR1−/− n = 46; TNFR2−/− n = 39. Mice were followed for 4 weeks following operation. All TNFR1−/− and TNFR2−/− ligated mice and ~50% WT ligated mice with premature death underwent autopsy to assess for blood in the chest cavity as an indicator of LV rupture.

Echocardiography

Under tribromoethanol sedation, echocardiography was performed at baseline and 4 weeks using a Philips Sonos 5500, 15 MHz linear array transducer. Measurements included left ventricular (LV) end-diastolic (ED) and end-systolic (ES) diameter (D), wall thickness, and end-diastolic and end-systolic volume (V) using the modified Simpson's method.

LV pressure measurement

In a subset of mice, LV catheterization was performed 4 weeks after operation as previously described [10] using a Millar 1.4 Fr pressure catheter (Model SPR-835) inserted retrograde via the right carotid artery. Systolic function was indexed by dP/dt_{max} and dP/dt_{max} normalized for instantaneous LV pressure (IP). Diastolic function was assessed by LVEDP and tau, the time constant of LV relaxation, determined from the regression of dP/dt versus LV pressure.

Tissue harvest

Following the final study, mice were given sodium pentobarbital (50 mg/kg IP). The hearts were arrested in diastole with IV KCl, rapidly excised, and rinsed in ice-cold physiological saline. A short-axis LV section was formalin-fixed for 16 h, dehydrated in ethanol, and paraffin-embedded for histological studies. The remaining LV was separated into infarcted (scar) and non-infarcted regions, snap-frozen in liquid nitrogen, and stored at −80°C. Unless otherwise specified, non-infarcted tissue was used for molecular analyses.

Cell culture and transfection

H9c2 cells (ATCC) were seeded in 100 mm tissue culture dishes and transfected for 24 h with the plasmid DNA (5μg/dish) using Transfectin® transfection reagent (BioRad). Briefly, 10 μL of Transfectin was added to 500μL of serum free DMEM media followed by the addition of plasmid DNA. The mixture was incubated for 15 min at room temperature prior to adding it onto the cells. In specific protocols, cells were also treated with 20ng/mL of either recombinant mouse TNF or IL-1β (BD Biosciences) for different time periods as indicated.

Construction of expression plasmids

Expression plasmids for NF-κB subunits p65 and p50 were purchased from Panomics. Full length mouse TNFR2 cDNA was amplified by PCR from mouse aortic endothelial cell RNA using the following primers; forward 5′- CACCGCCACCGCTGCCCCTATG-3′, reverse 5′-GTCAGGGGTCAGGCCACTTT-3′. The cDNA was cloned into pcDNA3.1-TOPO expression plasmid (Invitrogen) and its sequence verified. Truncated TNFR1 expression constructs (TNFR1Δ205 and TNFR1Δ244) were generous gifts from Drs. Wang Min and Jordan Pober, Yale University [11].

Western immunoblotting

Total protein extraction, SDS-PAGE Western blotting, and immunodetection using electro-chemiluminescence (ECL) were performed as previously described [10,12,13].

Electrophoretic mobility shift assay (EMSA)

NF-κB DNA binding activity was quantified by EMSA as previously described [12]. To determine NF-κB subunit composition, we performed gel supershift assays. Nuclear protein (10 μg) was preincubated for 40 min on ice with antibodies against the NF-κB subunits - p65, p50, p52, cRel, or Rel B (1 μg, Santa Cruz) or control IgG (1 μg) prior to the addition of the ^{32}P-labeled double stranded consensus oligonucleotide.

Quantitative real-time PCR

Total RNA was isolated from LV tissue using TRIzol reagent (Invitrogen), and cDNA was synthesized from 1 μg RNA using the iScript™ cDNA Synthesis kit (BioRad). Relative levels of mRNA transcripts for atrial natriuretic factor (ANF), connective tissue growth factor (CTGF), TNF, interleukin(IL)-1β, IL-6, IL-10, matrix metalloproteinase(MMP)-2, and MMP-9 were quantified by real-time PCR using SYBR® Green (Applied Biosystems). Data

were normalized to GAPDH expression using the C_T comparative method [14]. Primer pairs are listed in Supplemental Table 1.

Histology and immunohistochemistry

H&E and Masson's trichrome stains were used to determine cardiomyocyte cross-sectional area and myocardial fibrosis. Immunostaining for malondialdehyde(MDA)-adducted proteins was performed using anti-MDA antibody (Academy Bio-Med) as previously described [13]. Activated macrophages were detected by rat anti-mouse MOMA-2 monoclonal antibody (Chemicon). Immunoreactivity was quantitated from at least 20 random fields by light microscopy. Apoptosis was assessed by terminal deoxytransferase-mediated dUTP nick-end labeling (TUNEL) using an APO-BrdU TUNEL Assay (Invitrogen). Sections were also co-stained with DAPI (Invitrogen) to identify nuclei, and mouse anti-α-actinin conjugated with TRITC (abcam) to identify myocytes. Images were recorded using a Zeiss SM510 inverted confocal scanning laser microscope.

Statistical Analysis

Several statistical techniques were employed. For two-group comparisons, we used the unpaired two sample t test. For comparisons of more than two groups, we used one-way ANOVA if there was one independent variable (e.g., genotype alone), two-way ANOVA if there were two independent variables (e.g., genotype and ligation status), and two-way repeated measures ANOVA for matched observations over time with two independent variables. To adjust for multiple comparisons, we performed Student-Newman-Keuls post-test, which maintains overall Type I error (α) at 5%. Pair-wise comparisons were made between sham groups across genotypes, sham versus HF within each genotype, and HF groups across genotypes. A p value of < 0.05 was considered significant.

Animal survival was evaluated by the Kaplan-Meier method, and the log-rank test was used to compare survival curves between WT sham and WT HF as well as between WT HF and TNFR1−/− and TNFR2−/− HF (testing three null hypotheses). Multiple testing Bonferroni adjustment was performed manually and a p value of < 0.0167 (0.05/3) was considered significant. Continuous data are summarized as mean ± SD.

RESULTS

TNFR1 and TNFR2 differentially modulate post-infarction remodeling

Echocardiography revealed no baseline differences in LV wall thickness or systolic function between WT, TNFR1−/−, and TNFR2−/− mice (Supplemental Table 2). TNFR2−/− mice had a mild increase in LV size over WT, consistent with the ~15% greater body weight of these animals. In comparison to sham operated mice, WT mice at 28 days post-infarction exhibited significantly increased lung, right ventricular (RV), and liver weight normalized for tibia length (TL), consistent with pulmonary and systemic congestion that are hallmarks of HF (sham vs. HF, mg/mm: lung/TL, 6.7 ± 1.1 vs. 7.7 ± 2.5, $p < 0.05$; RV/TL, 1.0 ± 0.3 vs. 1.3 ± 0.4, $p < 0.005$; liver/TL, 52.2 ± 8.0 vs. 57.0 ± 8.2, $p < 0.05$). Kaplan-Meier survival curves (Figure 1A) revealed significantly increased HF mortality over sham for each genotype at 28 days post-infarction. Deficiency of either TNFR imparted a survival benefit over WT HF, primarily occurring in the first week post-infarction. In this time frame after coronary ligation, cardiac rupture is the main cause of death and is associated with MMP-2 and MMP-9 activation [15, 16]. In WT HF, the incidence of LV rupture was 45%, whereas no rupture was seen in either TNFR1−/− or TNFR2−/− HF mice. Moreover, at 4 weeks post-infarction, there was markedly increased MMP-2 and MMP-9 gene expression in WT non-infarcted myocardium over sham, whereas there was no such upregulation in TNFR1−/− or TNFR2−/− HF hearts (Supplemental Figure 1). Also, in the infarct scar, TNFR1−/− and TNFR2−/− HF exhibited significantly

attenuated MMP-2 and MMP-9 expression compared to WT HF. These results suggested that signaling via both TNFR1 and TNFR2 contributes to MMP induction and cardiac rupture after coronary ligation in mice.

In WT failing hearts (non-infarcted myocardium), TNFR1 and TNFR2 protein increased 1.5-fold and 1.3-fold, respectively, over sham (Figure 1B). In TNFR2−/− HF, TNFR1 also increased 1.5-fold, analogous to WT. However, in TNFR1−/− HF, there was no change in TNFR2. Figure 1C depicts LV tissue sections, M-mode echocardiograms, and corresponding group data. With HF, there was LV dilatation (increased LVEDV and LVESV) and systolic dysfunction (reduced LVEF) regardless of genotype. However, compared to WT HF, LV dilatation was attenuated in TNFR1−/− HF and exaggerated in TNFR2−/− HF. LVEF was also improved in TNFR1−/− HF; however, it was not different in TNFR2−/− HF, despite the larger chamber volumes. Differences in LV remodeling occurred despite equivalent infarct size in WT, TNFR1−/−, and TNFR2−/− HF, indicating divergent responses in the remote (non-infarcted) and border zones.

TNFR1 and R2 have divergent effects on inotropy but cooperatively impair lusitropy in HF

Figure 2 shows representative LV pressure and dP/dt traces from WT sham, and WT, TNFR1 −/−, and TNFR2−/− HF. Summary hemodynamic data from all groups are shown in the Table. WT failing hearts exhibited marked systolic and diastolic dysfunction over sham with reduced HR, LVSP, dP/dt_{max}, dP/dt_{max}/IP, and increased LVEDP and tau. TNFR1−/− HF displayed uniform improvements in these parameters compared to WT HF, indicating better contractility and lusitropy. Interestingly, despite exaggerated remodeling, TNFR2−/− HF exhibited a mixed mechanical response. LVSP, dP/dt_{max}, and dP/dt_{max}/IP were markedly depressed, comparable to WT HF. However, LVEDP and tau, indicators of diastolic performance, were much improved over WT HF. Taken together, this indicated that whereas TNFR1 deficiency in HF resulted in global improvement in systolic and diastolic function, TNFR2 deficiency exaggerated structural remodeling but still improved diastolic properties, thereby moderating changes in LV performance.

TNFR1 and TNFR2 differentially modulate cardiac hypertrophy and fibrosis in HF

Failing hearts from each HF group exhibited increased LV mass/TL ratio as compared to sham, consistent with LV hypertrophy (Figure 3A). Compared to WT HF, the LV/TL ratio was lower in TNFR1−/− HF and higher in TNFR2−/− HF. ANF gene expression by RT-PCR (Figure 3B) also revealed increased, and comparable, expression in WT and TNFR2−/− HF compared to TNFR1−/− HF (which was not significantly increased over TNFR1−/− sham). Consistent with the gravimetric data, histological assessment revealed larger myocyte area in all HF groups as compared to sham, but the degree of hypertrophy was attenuated in TNFR1−/− HF and enhanced in TNFR2−/− HF (Figure 3C). These results suggested that in HF, TNFR1 is pro-hypertrophic whereas TNFR2 is anti-hypertrophic.

Collagen deposition in non-infarcted myocardium (remote and border zones) was significantly augmented in the failing heart (Figure 3D). The degree of fibrosis was attenuated in TNFR1 −/− HF as compared to either WT or TNFR2−/− HF, both of which exhibited equivalent increases in fibrosis. Similar responses were seen for gene expression of CTGF, a pro-fibrotic matrix-associated protein (Figure 3F). Notably, as compared to WT HF, border zone collagen was attenuated in TNFR1−/− HF mice but exaggerated in TNFR2−/− HF mice (Figure 3E). The pattern of remote zone collagen deposition was similar to total collagen deposition. This suggested that changes in border zone fibrosis in TNFR2−/− mice may have influenced scar stability and contributed to improvements in LV diastolic performance and survival over WT HF, despite exaggerated chamber dilatation and hypertrophy.

TNFR1 and TNFR2 induce divergent NF-κB signaling responses in HF

EMSA revealed marked NF-κB activation in failing myocardium (Figure 4A), and gel supershifts revealed that p65 was the primary NF-κB subunit, with a minor contribution from RelB and negligible p50, p52, and cRel. A similar supershift pattern was seen in both TNFR1 −/− and TNFR2−/− HF hearts (data not shown). As seen in Figure 4B, WT failing hearts exhibited a robust (> 2-fold) increase in NF-κB DNA binding as compared to sham. Moreover, there was significant attenuation of NF-κB activation in TNFR1−/− HF and, conversely, exaggeration of NF-κB activity in TNFR2−/− HF.

Cardiac gene expression (by RT-PCR) of pro-inflammatory TNF, IL-1β, and IL-6 and the anti-inflammatory IL-10 in was markedly increased in WT HF as compared to sham (Figure 4C). This increase was either absent or attenuated in TNFR1−/− HF suggesting a generalized reduction of inflammatory responses upon loss of TNFR1 in HF. In TNFR2−/− HF, the upregulation of pro-inflammatory cytokines was either comparable to (TNF) or augmented over (IL-1β and IL-6) WT HF, whereas there was no increase at all in anti-inflammatory IL-10. These results paralleled the changes in NF-κB as TNF, IL-1β and IL-6 are regulated by NF-κB and as IL-10 is a known suppressor of NF-κB activation. Moreover, as compared to sham, there was increased MOMA-2 staining for activated macrophages in the myocardium of TNFR2−/− HF ($p < 0.05$) and a trend toward increased staining in WT HF, but no change in TNFR1−/− HF (Figure 4D). TNFR2−/− HF also exhibited more activated macrophages as compared to TNFR1−/− HF ($p < 0.05$). TNF-mediated activation of either JNK or p38 MAPK can also induce significant pro-inflammatory effects. WT HF exhibited augmented p38 MAPK and JNK2 phosphorylation over WT sham, both of which were attenuated in TNFR1−/− HF (Figure 4E). In TNFR2−/− HF, p38 MAPK phosphorylation was exaggerated, paralleling NF-κB activity, whereas JNK2 phosphorylation was comparable to WT HF. Taken together, these results indicate moderation and exacerbation of the HF-associated pro-inflammatory state upon loss of TNFR1 or TNFR2, respectively.

Sustained NF-κB activation is pro-apoptotic in H9c2 cardiomyocytes, an effect modulated by TNFR1

In these studies, apoptosis was indexed by levels of cleaved poly-ADP ribose polymerase (PARP) and caspase-3. As shown in Figure 5A, TNF induced rapid IκBα degradation in H9c2 cells, with the appearance of newly synthesized IκBα within 1 h, indicating transient NF-κB activation. There was no apoptosis, indicated by predominantly uncleaved PARP (upper band). In contrast, pre-treatment with the protein synthesis inhibitor cycloheximide (CHX) before TNF prevented IκBα resynthesis and induced apoptosis (augmented cleaved PARP). Although the mechanism commonly invoked for TNF-induced apoptosis with CHX is the prevention of synthesis of NF-κB-responsive anti-apoptotic proteins [15,25], protein expression of NF-κB-responsive Bcl-X_L and the Bcl-X_L/Bax ratio did not change (Figure 5B). In contrast, inhibition of NF-κB nuclear translocation by the peptide SN50 attenuated apoptosis (Figure 5C), suggesting that sustained NF-κB activity was itself contributing to cell death. Moreover, selective overexpression of p65 and/or p50 for 24 h augmented PARP and caspase-3 cleavage, regardless of TNF exposure (Figure 5D), and the pro-apoptotic effect of p65 overexpression exhibited dose-dependency (Figure 5E). Overexpression of p65 and/or p50 did not alter the expression of a range of pro-and anti-apoptotic proteins including TRAF-1 and 2, Fas and FasL, Bax and BCL_{XL}, cFLIP and cIAP, and p53 (Figure 5F), indicating separate, as of yet undetermined, mechanisms of NF-κB-induced cardiomyocyte apoptosis.

TNFR1 deletion mutants that lack most (TNFR1Δ244) or all (TNFR1Δ205) of the TNFR1 cytoplasmic domain [12], as well as full-length, normally functional TNFR2 were overexpressed under similar conditions. TNFR1Δ205 was highly effective (and better than TNFR1Δ244) in abrogating NF-κB activation in response to TNF but not to IL-1β (Figure 6A).

As shown in Figure 6B, the pro-apoptotic effects of p65 and p50 overexpression were markedly attenuated upon TNFR1Δ205 co-transfection (indicated by diminished PARP and caspase-3 cleavage). TNFR1Δ205 overexpression also blunted the increase in IκBα, an NF-κB responsive gene. Hence, NF-κB-induced apoptosis depends in part on TNF induction and TNFR1 downstream signaling. Conversely, TNFR2 overexpression dose-dependently reduced TNF-induced NF-κB activation (Figure 6C), consistent with the *in vivo* responses in HF (Figure 4). Co-transfection with both p65 and TNFR2 did not, however, reduce PARP cleavage and apoptosis in H9c2 cardiomyocytes (Figure 6D), suggesting that TNFR2 is a weaker modulator of NF-κB-induced apoptosis than TNFR1. This may not, however, fully represent the *in vivo* situation, given the complex binding properties of TNFR2 to membrane-bound and soluble TNF (mTNF and sTNF, respectively), and the importance of juxtacrine interactions among different cell types in HF.

TNFR1 and TNFR2 induce divergent apoptotic effects but similar oxidative stress responses in the failing heart

Apoptosis, inflammation, and oxidative stress are three key TNF-mediated responses that are independently linked to pathological remodeling. As our studies indicated that dichotomous NF-κB responses related to each TNFR could also differentially impact cell survival, we evaluated apoptosis in WT, TNFR1−/−, and TNFR2−/− sham and HF hearts and whether changes in apoptosis were associated with directionally similar changes in oxidative stress. TUNEL staining revealed that apoptosis was increased over sham only in WT and TNFR2−/− HF and not in TNFR1−/− HF (Figure 7A), consistent with the cell data demonstrating a pro-apoptotic effect of TNFR1. Remarkably, TNFR2−/− HF hearts exhibited exaggerated apoptosis over WT and TNFR1−/− HF indicating that TNFR2 confers (contrary to the cell studies) beneficial anti-apoptotic effects in the failing heart. As shown in Figure 7B, immunostaining revealed a significant ~2-fold increase in MDA modified proteins in WT HF compared to sham. However, despite the marked differences in remodeling between TNFR1−/− and TNFR2−/− HF, there were similar reductions in oxidative stress as compared to WT HF, suggesting that other factors such as apoptosis and inflammatory activation had primacy in the remodeling responses, and that the changes in inflammation and apoptosis were not solely epiphenomena related to a global improvement (or worsening) in LV remodeling.

DISCUSSION

There are several key findings of this study. First, TNFR1- and TNFR2-dependent signaling had unique effects on post-infarction remodeling *in vivo*, such that TNFR1 aggravated, whereas TNFR2 ameliorated, chamber remodeling and hypertrophy. Second, the impact on cardiac mechanics and survival were more complex: whereas TNFR1- and TNFR2-responses magnified and alleviated, respectively, LV systolic dysfunction, signaling through both receptors was necessary to increase post-infarction mortality (due to myocardial rupture) and to induce diastolic dysfunction. Third, TNFR1- and TNFR2-induced remodeling responses were accompanied by exacerbation and moderation of cardiac inflammation as assessed by NF-κB activation, inflammatory cytokine expression, p38 MAPK phosphorylation, and macrophage infiltration. Fourth, in H9c2 cardiomyocytes, TNFR1 augmented whereas TNFR2 moderated NF-κB activation and sustained NF-κB activation was pro-apoptotic in a TNFR1-dependent manner. Fifth, TNFR1 was pro-apoptotic and TNFR2 anti-apoptotic in the failing heart *in vivo*, whereas signaling via both receptors cooperatively augmented oxidative stress. Taken together, we have demonstrated complex pathophysiological responses in HF specific to each TNFR that are related in large part to disparate, opposing effects on NF-κB, inflammatory activation, and apoptosis. Analogous dichotomous TNFR-mediated responses in human HF may therefore help explain the unexpectedly negative results of clinical trials of global TNF blockade.

Although the "cytokine hypothesis" posits a uniformly detrimental effect of TNF in HF, TNF has bimodal effects on contractility [17] and is cardioprotective during acute stress [6–8]. As shown in Figure 1B and Figure 4C, TNF, TNFR1, and TNFR2 are all upregulated during the progression of remodeling in murine HF, indicating uniform enhancement of TNF signaling. This contrasts with end-stage human HF where TNF levels are high but both TNFRs are downregulated [18]. Exacerbation of LV remodeling in TNFR2−/− HF mice occurred despite similar degrees of upregulation of both TNF and TNFR1, suggesting that unique cardioprotective benefits are referable to TNFR2 in HF. Moreover, amelioration of remodeling in TNFR1−/− HF mice occurred without an increase in TNFR2 expression and despite persistent (though attenuated) TNF upregulation, suggesting that detrimental biological responses in HF are uniquely referable to TNFR1. Thus, our results demonstrate that TNFR1 promotes detrimental remodeling whereas TNFR2 is cardioprotective in HF with regard to chamber remodeling, systolic dysfunction, and hypertrophy.

These generalized effects on post-infarction remodeling notwithstanding, the complex functional interrelationship between the TNFRs in HF is evidenced by the cooperative, rather than divergent, effects of TNFR1 and TNFR2 on LV diastolic performance and survival, as loss of signaling via either TNFR improved diastolic function and mortality post-infarction. Prior studies have established that the most prevalent cause of death following infarction in mice is LV rupture (usually within the first week), that TNF directly contributes to cardiac rupture, and that this event is related to activation of MMPs, particularly MMP-2 and MMP-9, in the heart [15,16]. MMP-2 and MMP-9 activities increase by day 3, peak at day 7, and remain elevated to day 28 post-infarction [19]. In our study, early LV rupture was prevented in both TNFR1−/− and TNFR2−/− HF mice, with both groups exhibiting less infarct and non-infarct zone MMP-2 and MMP-9 expression at 28 days as compared to WT HF. This suggested that analogous MMP modulation with loss of either TNFR1 or TNFR2 function was also occurring at earlier time points after infarction, offering one potential mechanism for the reduced mortality in TNFR1−/− and TNFR2−/− mice. Hence, joint functionality of both TNF receptors was required for LV rupture to occur in the early post-infarction period. Notably, this mortality benefit was independent of the subsequent effects of TNFR1 and TNFR2 on LV remodeling. However, we speculate that the divergent TNFR-specific effects on progressive LV remodeling would secondarily impact mortality over extended periods of time after scar stabilization.

As there was improved global remodeling in TNFR1−/− HF, accompanying improvements in diastolic function would be expected with TNFR1 deficiency. Indeed, there were generalized reductions in CTGF expression and cardiac fibrosis in TNFR1−/− HF hearts, which would favorably influence LV diastolic properties. More difficult to reconcile is the maintenance of diastolic function in TNFR2−/− HF mice despite worsening of chamber remodeling. As LV rupture was abrogated in these mice, these effects may be related to improved scar mechanics and/or border zone stability. Indeed, although the overall extent of cardiac fibrosis was similar in TNFR2−/− and WT HF, there was greater border zone collagen deposition that can potentially better resist rupture and favorably influence diastolic performance. However, it is important to recognize that the degree and distribution of myocardial fibrosis may itself also be influenced by altered global/regional wall stress, and whether the changes in connective tissue composition are a cause or consequence of altered chamber diastolic properties and wall stress is difficult to resolve with our experimental design.

A key finding of our study is that TNFR1 and TNFR2 had directionally opposite effects on NF-κB and inflammation in HF, and that these events contributed to the differences in LV remodeling. TNFR1 recruits adaptor proteins via its death domain to trigger TRAF2-dependent signaling that activates NF-κB, JNK, and p38 MAPK [9,20]. TNFR2 can also activate NF-κB, JNK, and p38 MAPK via direct TRAF2 binding. TNF can also induce apoptosis via either TNFR and trigger the generation of reactive oxygen species (ROS) [9,20]. We observed robust

myocardial NF-κB activation in HF that was due almost entirely to p65. The failing heart also exhibited significant p38 and JNK2 activation, both of which have significant pro-inflammatory effects [21,22], upregulation of pro-inflammatory TNF, IL-1β, IL-6 and anti-inflammatory IL-10, and enhanced tissue infiltration of activated macrophages, albeit at low absolute levels. Hence, there was a pro-inflammatory state in WT HF, consistent with prior studies [1,18,23]. In TNFR1−/− HF there was attenuation of NF-κB activation, p38 and JNK phosphorylation, and TNF, IL-1β, IL-6 and IL-10 expression as compared to WT HF, and no significant activated macrophage infiltration as compared to TNFR1−/− sham. In contrast, TNFR2−/− HF hearts exhibited greater NF-κB activation, p38 MAPK phosphorylation, and IL-1β and IL-6 expression, and less anti-inflammatory IL-10 expression compared to WT HF, and greater activated macrophage infiltration than TNFR1−/− HF. Thus, our data establish that in chronic HF, TNFR1 is proinflammatory whereas TNFR2 is anti-inflammatory. Moreover, the sharp divergence of TNFR1 and TNFR2 effects on downstream mediators suggests that although acute signaling via the TNFRs may overlap significantly, TNFR crosstalk is much less prominent in chronic HF, leading to dichotomous downstream TNF responses.

Although NF-κB is chronically activated in HF [24], whether this is protective or detrimental is unclear. In addition to stimulating inflammation, NF-κB upregulates both anti-apoptotic and pro-apoptotic genes [9,20,25], and can potentially induce either survival or death. Our cell studies indicate that p65 and/or p50 overexpression is pro-apoptotic in H9c2 cardiomyocytes via a mechanism that appears independent of changes in classical pro-and anti-apoptotic gene expression. Moreover, analogous to *in vivo* HF, TNFR1 increased whereas TNFR2 blunted NF-κB activation. Importantly, the pro-apoptotic effects of NF-κB overexpression required TNF elaboration and concomitant TNFR1 signaling, but was not modified by TNFR2 overexpression. As HF is characterized by increases in both TNF/TNFRs and NF-κB, analogous functional interrelationships between TNFR1 and NF-κB may also occur in the failing heart. Indeed, evaluation of apoptotic rates revealed that in TNFR1−/− HF, attenuated NF-κB activation was paralleled by reduced myocardial apoptosis as compared to WT HF, whereas the opposite response was seen in TNFR2−/− HF. Augmented myocardial TNF expression has been shown to increase oxidative protein modifications in the heart [26]. However, oxidative stress, as indexed by protein-MDA adducts, was equally reduced in both TNFR1−/− and TNFR2−/− HF, suggesting that the changes in cell survival were not simply epiphenomena accompanying global directional changes in remodeling. Hence, sustained changes in NF-κB activation are likely to underlie many of the divergent remodeling responses related to each TNFR. Indeed, recent studies indicate that post-infarction remodeling is attenuated in p50 null mice [27,28]. However, as our data show that NF-κB in the murine failing heart is almost entirely p65, further studies are required to define the relevance of these findings.

Our results extend as well as contrast with recent work in this area by others [29,30]. Ramani et al [29] also reported improved remodeling and survival in TNFR1−/− mice post-infarction over WT, but no differences in TNF and IL-1β expression. Recently, after our original presentation of these data [31], Monden et al [30] reported that TNFR1 ablation improved but TNFR2 ablation exacerbated post-infarct remodeling and IL-1β and IL-6 expression. Although these general conclusions are the same, there are also significant differences from our study, which establishes more complex effects of TNFR1 and TNFR2 in HF. Monden et al did not observe a post-infarction mortality benefit in TNFR2−/− mice or differences in LV rupture in either TNFR1−/− or TNFR2−/− mice. Moreover, we observed multifaceted hemodynamic responses in our study, with improved LV diastolic performance in TNFR2−/− HF mice despite exaggerated structural remodeling. Also, unlike our results demonstrating a pro-hypertrophic and pro-fibrotic effect of TNFR1 in the failing heart, Monden et al reported no effects of TNFR1 on these parameters. While the reasons for these conflicting results are not fully clear, potential explanations include the older age of the mice and greater degrees of HF in WT mice (which

exhibited a two-fold higher LVEDP) in our study, and perhaps an analytical approach that afforded greater discrimination of subtler differences between the genotypes. Further studies will be needed to resolve this. Most importantly, however, we provide novel mechanistic data that link in vivo remodeling to the primary downstream signaling pathways activated by TNF in the failing heart (particularly NF-kB), as well as to alterations in apoptosis and oxidative stress, and characterize the interrelationship between TNFR1, TNFR2, NF-kB, and cell survival. Indeed, our results indicate for the first time an opposing relationship between TNFR1 and TNFR2 and the activation of NF-kB in HF, and help provide a more comprehensive and mechanistic basis for TNFR-specific remodeling responses.

In summary, TNF induces dichotomous effects in HF that are directly referable to its two membrane receptors, and occur (at least in part) as a result of disparate effects on the critical downstream mediator NF-κB, inflammatory signaling responses, and apoptosis. The overall balance between these opposing receptor-specific responses in turn determines the ultimate impact of TNF on the HF phenotype. Hence, these results provide a potential explanation for the failure of the anti-TNF clinical trials, and, as a corollary, suggest that selective targeting of the individual TNFRs (TNFR1 blockade and/or TNFR2 augmentation) represents a better therapeutic approach in HF.

Clinical Impact Commentary

Despite the seminal observation that tumor necrosis factor-α (TNF) is an important mediator of pathological left ventricular remodeling in heart failure (HF), this discovery has not resulted in the development of new, effective treatments. On the contrary, the unexpected failure of clinical trials of global TNF blockade cast doubt as to the precise roles of inflammatory activation in general and of TNF in particular in the progression of chronic HF. As there are two cell-surface receptors for TNF (TNFR1 and TNFR2), we evaluated the remodeling responses specifically referable to each TNF receptor in chronic ischemic HF *in vivo* using TNFR1 and TNFR2 null mice. Our results indicate that TNF induces dichotomous effects in HF such that TNFR1 aggravated, whereas TNFR2 ameliorated, chamber remodeling and hypertrophy. Moreover, these effects occurred, at least in part, due to divergent effects on the activation of the downstream signaling mediator nuclear factor-κB, the regulation of inflammatory cytokines, and the induction of apoptosis: TNFR1 exacerbated, whereas TNFR2 ameliorated, these events. These results suggest that the overall balance between these opposing receptor-specific responses determines the ultimate impact of TNF on the HF phenotype, and that analogous TNF receptor-specific effects in human HF should be considered when developing anti-TNF therapies. Dichotomous TNFR-specific effects may also provide one explanation for the failure of the anti-TNF clinical trials. Selective targeting of the individual TNFRs (TNFR1 blockade and/or TNFR2 augmentation) may represent a better therapeutic approach in HF.

Supplementary Material

Refer to Web version on PubMed Central for supplementary material.

Acknowledgments

FUNDING SOURCES

This work was supported by a VA Merit Award and NIH grants ES11860, HL078825, and HL065660.

REFERENCES

1. Mann DL. Inflammatory mediators and the failing heart: past, present, and the foreseeable future. Circ Res 2002;91:988–998. [PubMed: 12456484]
2. Bozkurt B, Kribbs SB, Clubb FJ, Michael LH, Didenko VV, Hornsby PJ, Seta Y, Oral H, Spinale FG, Mann DL. Pathophysiologically relevant concentrations of tumor necrosis factor-α promote progressive left ventricular dysfunction and remodeling in rats. Circulation 1998;97:1382–1391. [PubMed: 9577950]
3. Li YY, Feng YQ, Kadokami T, McTiernan CF, Draviam R, Watkins SC, Feldman AM. Myocardial extracellular matrix remodeling in transgenic mice overexpressing tumor necrosis factor-α can be modulated by anti-tumor necrosis factor-α therapy. Proc Natl Acad Sci USA 2000;97:12746–12751. [PubMed: 11070088]
4. Moe GW, Marin-Garcia J, Konig A, Goldenthal M, Lu X, Feng Q. In vivo TNF-α inhibition ameliorates cardiac mitochondrial dysfunction, oxidative stress, and apoptosis in experimental heart failure. Am J Physiol Heart Circ Physiol 2004;287:1813–1820.
5. Iversen PO, Nicolaysen G, Sioud M. DNA enzyme targeting TNF-α mRNA improves hemodynamic performance in rats with postinfarction heart failure. Am J Physiol Heart Circ Physiol 2001;281:H2211–H2217. [PubMed: 11668085]
6. Kurrelmeyer K, Michael L, Baumgarten G, Taffet G, Peschon J, Sivasubramanian N, Mann DL. Endogenous myocardial tumor necrosis factor protects the adult cardiac myocyte against ischemic-induced apoptosis in a murine model of acute myocardial infarction. Proc Natl Acad Sci USA 2000;290:5456–5461. [PubMed: 10779546]
7. Skyschally A, Gres P, Hoffmann S, Haude M, Erbel R, Schulz R, Heusch G. Bidirectional role of tumor necrosis factor-α in coronary microembolization: progressive contractile dysfunction versus delayed protection against infarction. Circ Res 2007;100:140–146. [PubMed: 17170366]
8. Wada H, Saito K, Kanda T, Kobayashi I, Fujii H, Fujigaki S, Maekawa N, Takatsu H, Fujiwara H, Sekikawa K, Seishima M. Tumor necrosis factor-α (TNF-α) plays a protective role in acute viral myocarditis in mice: A study using mice lacking TNF-α. Circulation 2001;103:743–749. [PubMed: 11156888]
9. Aggarwal BB. Signalling pathways of the TNF superfamily: a double-edged sword. Nat Rev Immunol 2003;3:745–756. [PubMed: 12949498]
10. Luo J, Hill BG, Gu Y, Cai J, Srivastava S, Bhatnagar A, Prabhu SD. Mechanisms of acrolein-induced myocardial dysfunction: implications for environmental and endogenous aldehyde exposure. Am J Physiol Heart Circ Physiol 2007;293:H3673–H3684. [PubMed: 17921335]
11. Zhang H, Zhang R, Luo Y, D'Alessio A, Pober JS, Min W. AIP1/DAB2IP, a novel member of the Ras-GAP family, transduces TRAF2-induced ASK1-JNK activation. J Biol Chem 2004;279:44955–44965. [PubMed: 15310755]
12. Chandrasekar B, Marelli-Berg FM, Tone M, Bysani S, Prabhu SD, Murray DR. Isoproterenol induces interleukin-18 expression via β2-AR, PI3 kinase, Akt, IκB kinase, and nuclear factor-κB signaling. Biochem Biophys Res Commun 2004;319:304–311. [PubMed: 15178407]
13. Srivastava S, Chandrasekar B, Gu Y, Luo J, Hamid T, Hill BG, Prabhu SD. Downregulation of CuZn-superoxide dismutase contributes to β-adrenergic receptor-mediated oxidative stress in the heart. Cardiovasc Res 2007;74:445–455. [PubMed: 17362897]
14. Livak KJ, Schmittgen TD. Analysis of relative gene expression data using real-time quantitative PCR and the 2-DDCT method. Methods 2001;25:402–408. [PubMed: 11846609]
15. Sun M, Dawood F, Wen WH, Chen M, Dixon I, Kirshenbaum LA, Liu PP. Excessive tumor necrosis factor activation after infarction contributes to susceptibility of myocardial rupture and left ventricular dysfunction. Circulation 2004;110:3221–3228. [PubMed: 15533863]
16. Matsumura S, Iwanaga S, Mochizuki S, Okamoto H, Ogawa S, Okada Y. Targeted deletion or pharmacological inhibition of MMP-2 prevents cardiac rupture after myocardial infarction in mice. J Clin Invest 2005;115:599–609. [PubMed: 15711638]
17. Prabhu SD. Cytokine-induced modulation of cardiac function. Circ Res 2004;95:1140–1153. [PubMed: 15591236]

18. Torre-Amione G, Kapadia S, Lee J, Durand J-B, Bies RD, Young JB, Mann DL. TNF-α and tumor necrosis factor receptors in the failing human heart. Circulation 1996;93:704–711. [PubMed: 8640999]
19. Mukherjee R, Mingoia JT, Bruce JA, Austin JS, Stroud RE, Escobar GP, McClister DM Jr, Allen CM, Alfonso-Jaume MA, Fini ME, Lovett DH, Spinale FG. Selective spatiotemporal induction of matrix metalloproteinase-2 and matrix metalloproteinase-9 transcription after myocardial infarction. Am J Physiol Heart Circ Physiol 2006;291:H2216–H2218. [PubMed: 16766634]
20. Wajant H, Pfizenmaier K, Scheurich P. Tumor necrosis factor signaling. Cell Death Differ 2003;10:45–65. [PubMed: 12655295]
21. Kyriakis JM, Avruch J. Mammalian mitogen-activated protein kinase signal transduction pathways activated by stress and inflammation. Physiol Rev 2001;81:807–869. [PubMed: 11274345]
22. Johnson GL, Nakamura K. The c-jun kinase/stress-activated pathway: regulation, function and role in human disease. Biochim Biophys Acta 2007;1773:1341–1348. [PubMed: 17306896]
23. Prabhu SD, Chandrasekar B, Murray DR, Freeman GL. β-Adrenergic blockade in developing heart failure: effects on myocardial inflammatory cytokines, nitric oxide, and remodeling. Circulation 2000;101:2103–2109. [PubMed: 10790354]
24. Wong SC, Fukuchi M, Melnyk P, Rodger I, Giaid A. Induction of cyclooxygenase-2 and activation of nuclear factor-κB in myocardium of patients with congestive heart failure. Circulation 1998;98:100–103. [PubMed: 9679714]
25. Luo JL, Kamata H, Karin M. IKK/NF-κB signaling: balancing life and death--a new approach to cancer therapy. J Clin Invest 2005;115:2625–2632. [PubMed: 16200195]
26. Canton M, Skyschally A, Menabò R, Boengler K, Gres P, Schulz R, Haude M, Erbel R, Di Lisa F, Heusch G. Oxidative modification of tropomyosin and myocardial dysfunction following coronary microembolization. Eur Heart J 2006;27:875–881. [PubMed: 16434410]
27. Frantz S, Hu K, Bayer B, Gerondakis S, Strotmann J, Adamek A, Ertl G, Bauersachs J. Absence of NF-κB subunit p50 improves heart failure after myocardial infarction. FASEB J 2006;20:1918–1920. [PubMed: 16837548]
28. Kawano S, Kubota T, Monden Y, Tsutsumi T, Inoue T, Kawamura N, Tsutsui H, Sunagawa K. Blockade of NF-κB improves cardiac function and survival after myocardial infarction. Am J Physiol Heart Circ Physiol 2006;291:H1337–H1344. [PubMed: 16632551]
29. Ramani R, Mathier M, Wang P, Gibson G, Tögel S, Dawson J, Bauer A, Alber S, Watkins SC, McTiernan CF, Feldman AM. Inhibition of tumor necrosis factor receptor-1-mediated pathways has beneficial effects in a murine model of postischemic remodeling. Am J Physiol Heart Circ Physiol 2004;287:H1369–H1377. [PubMed: 15317681]
30. Monden Y, Kubota T, Inoue T, Tsutsumi T, Kawano S, Ide T, Tsutsui H, Sunagawa K. Tumor necrosis factor-α is toxic via receptor 1 and protective via receptor 2 in a murine model of myocardial infarction. Am J Physiol Heart Circ Physiol 2007;293:H743–H753. [PubMed: 17416608]
31. Hamid T, Gu Y, Ortines RV, Luo J, Bhattacharya C, Xuan YT, Prabhu SD. Tumor necrosis factor (TNF) receptor1- and receptor2- dependent pathways differentially modulate post-infarction LV remodeling (abstract). Circulation 2005;112(17)II-850.

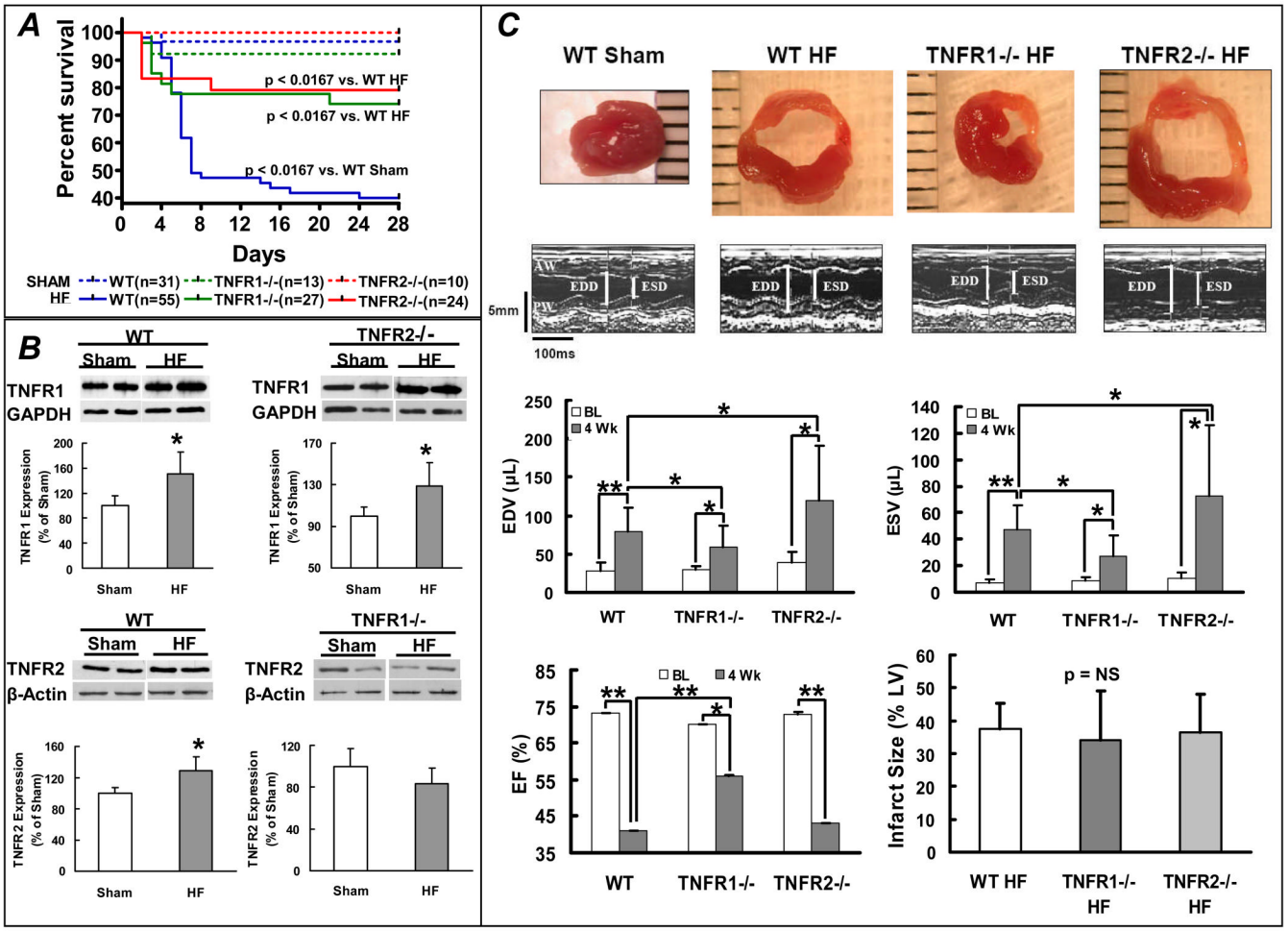

Figure 1.

TNFR1 and TNFR2 differentially modulate LV remodeling. *(A)* Kaplan-Meier survival curves from WT, TNFR1−/−, and TNFR2−/− mice after coronary ligation (HF) or sham operation. *(B)* Immunoblots and corresponding group data depicting changes in TNFR1 and TNFR2 expression in failing, remodeled myocardium. *p<0.05 vs. sham. *(C)* Short-axis LV sections, M-mode echocardiograms, and group data for LV function and infarct size from WT, TNFR1 −/−, and TNFR2−/− sham and HF mice. **p<0.005, *p<0.05.

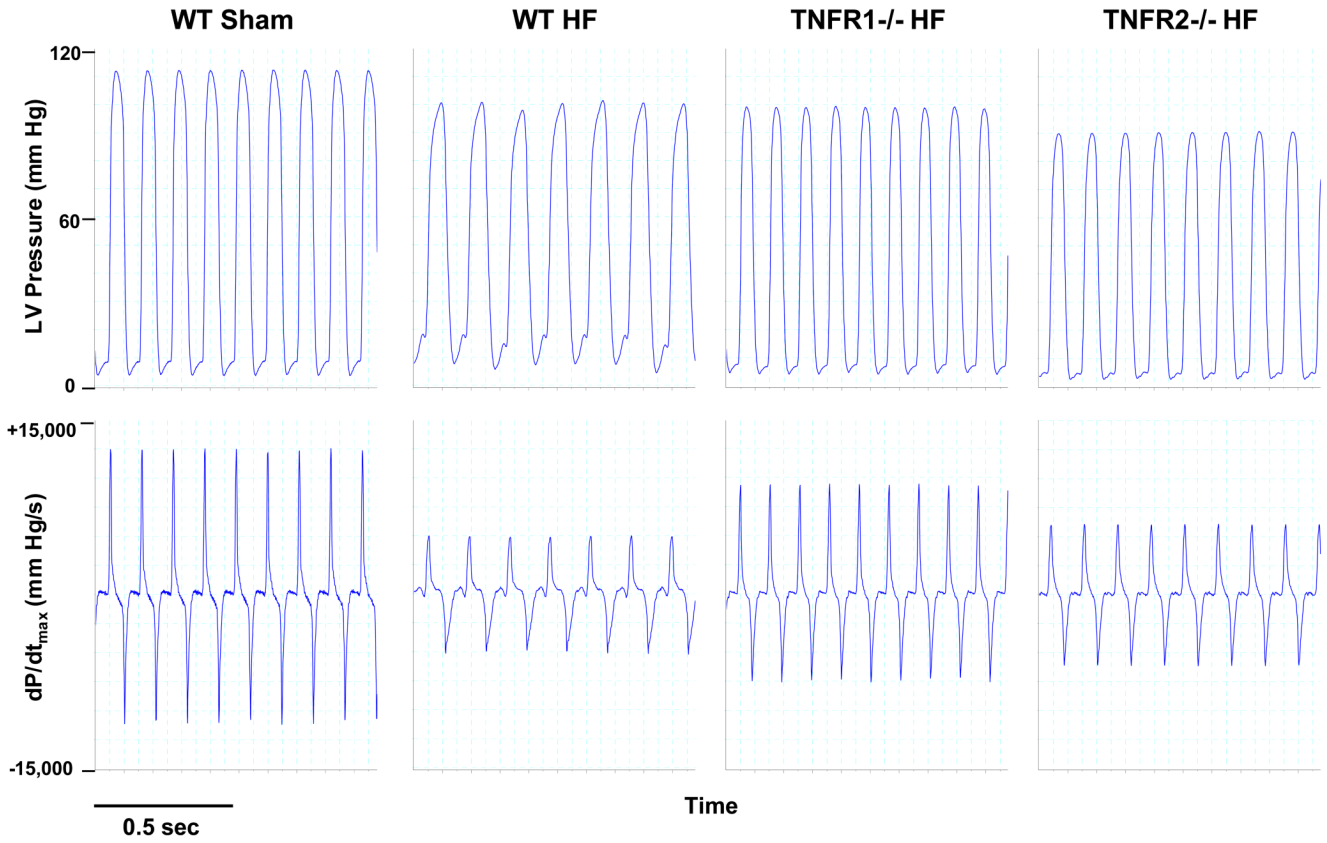

Figure 2.

Representative hemodynamic recordings for LV pressure and dP/dt_{max} from WT sham, WT HF, TNFR1−/− HF, and TNFR2−/− HF mice. LV peak pressure and dP/dt_{max} were depressed and LVEDP was elevated in WT HF. TNFR1−/− HF displayed global improvement in these parameters. TNFR2−/− HF exhibited similar reductions in dP/dt_{max} but improved LVEDP compared with WT HF.

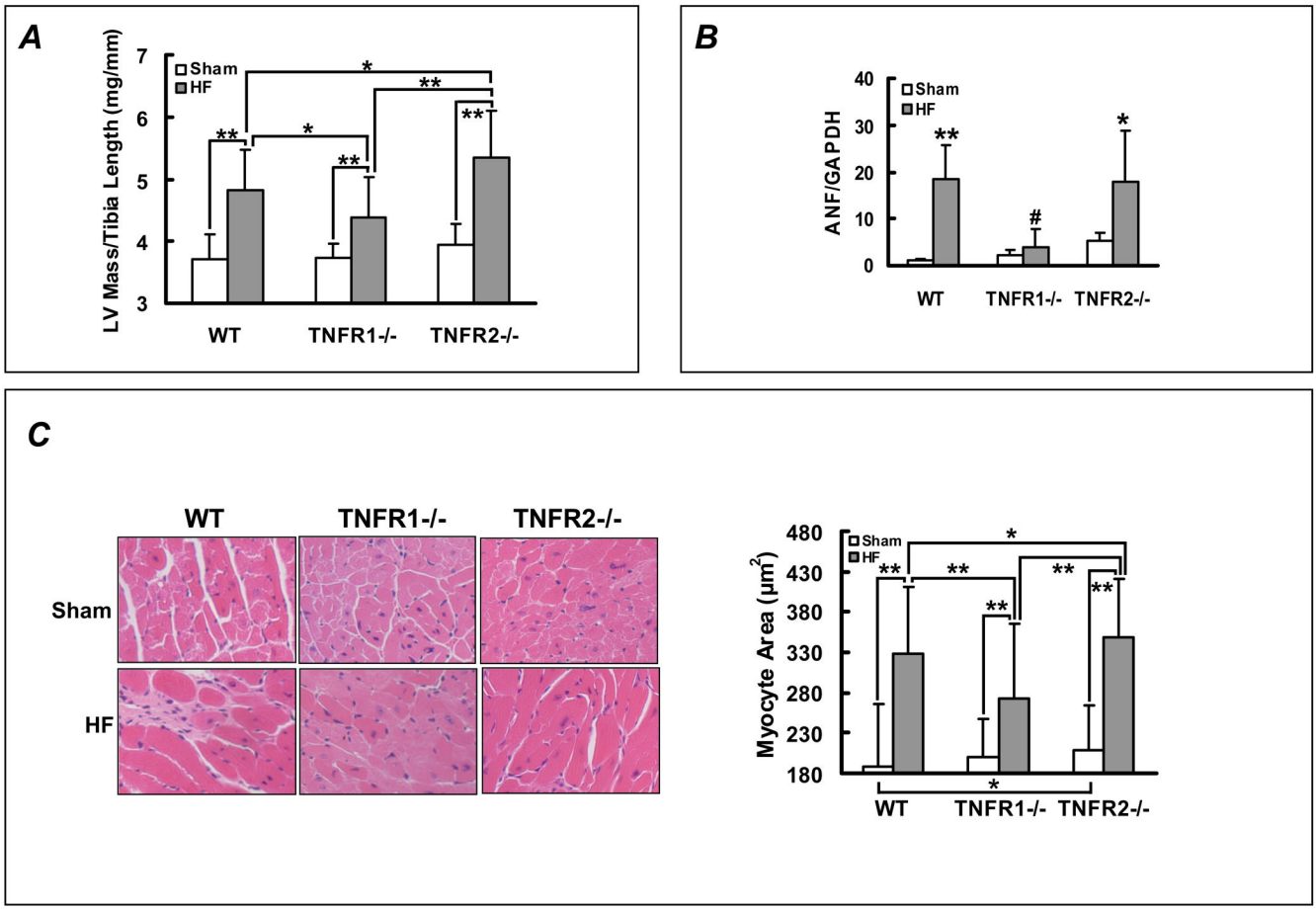

Figure 3A-C

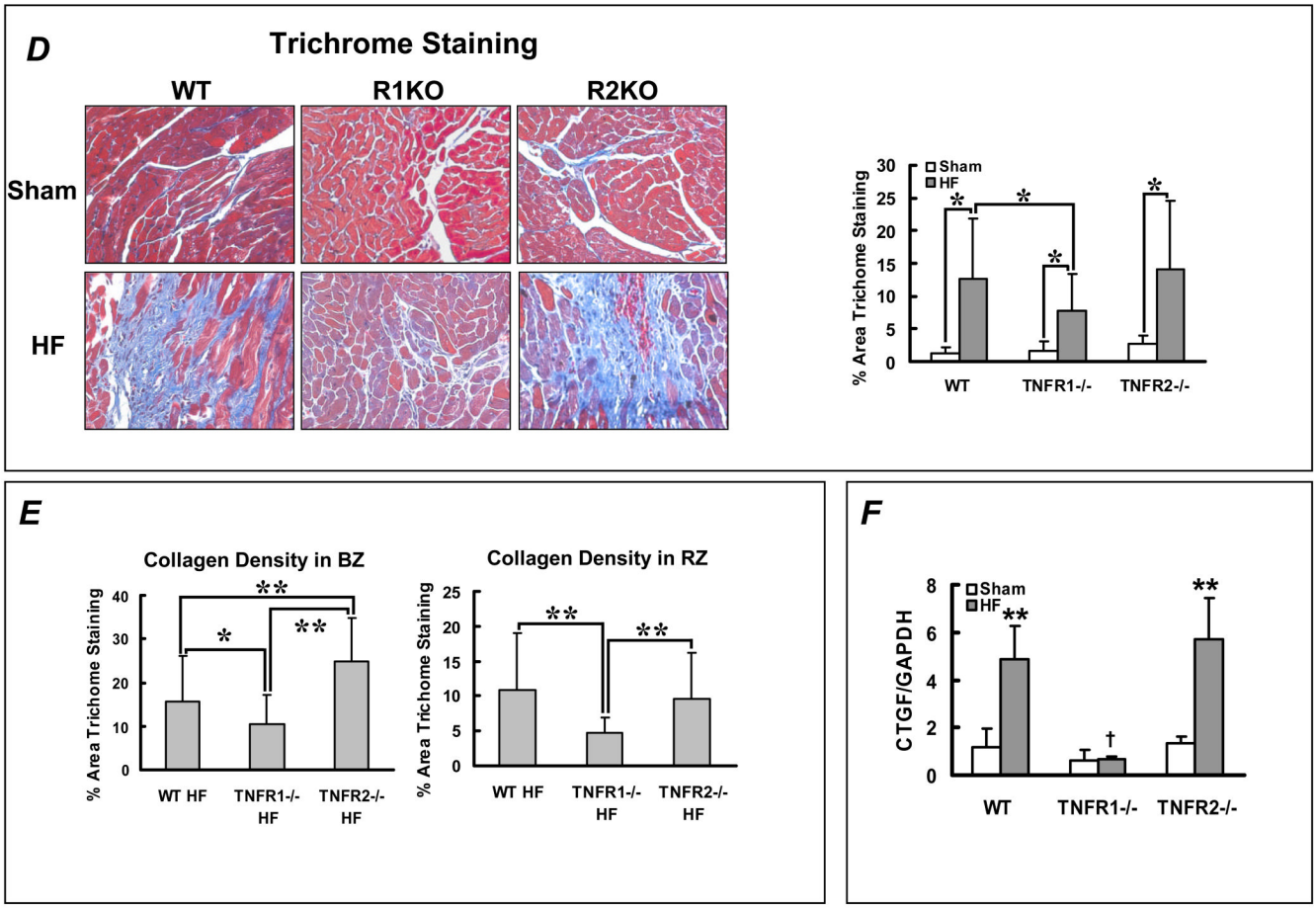

Figure 3D-F

Figure 3.

TNFR1- and TNFR2-specific effects on hypertrophy and fibrosis in HF. *(A)* LV mass/tibia length ratio from WT, TNFR1−/−, and TNFR2−/− sham and HF mice. **p<0.005, *p<0.05. *(B)* Normalized ANF gene expression from sham and failing myocardium by qRT-PCR analysis (n=4/group). **p<0.005, *p<0.05 vs. sham, #p<0.005 vs WT and TNFR2−/− HF. *(C)* Representative H&E histomicrographs of remodeled myocardium from each experimental group and quantitation of myocyte cross-sectional area. **p<0.0001, *p<0.05. *(D)* Masson's Trichrome stains and quantitation of fibrosis in non-infarcted myocardium (*i.e.*, remote and border zones). *p<0.05. *(E)* Selective border-zone (BZ) and remote-zone (RZ) fibrosis quantitation. **p<0.001, *p<0.05. *(F)* Normalized CTGF gene expression by qRT-PCR, **p<0.005 vs. sham; †p<0.005 vs WT and TNFR2−/− HF (n = 6/group).

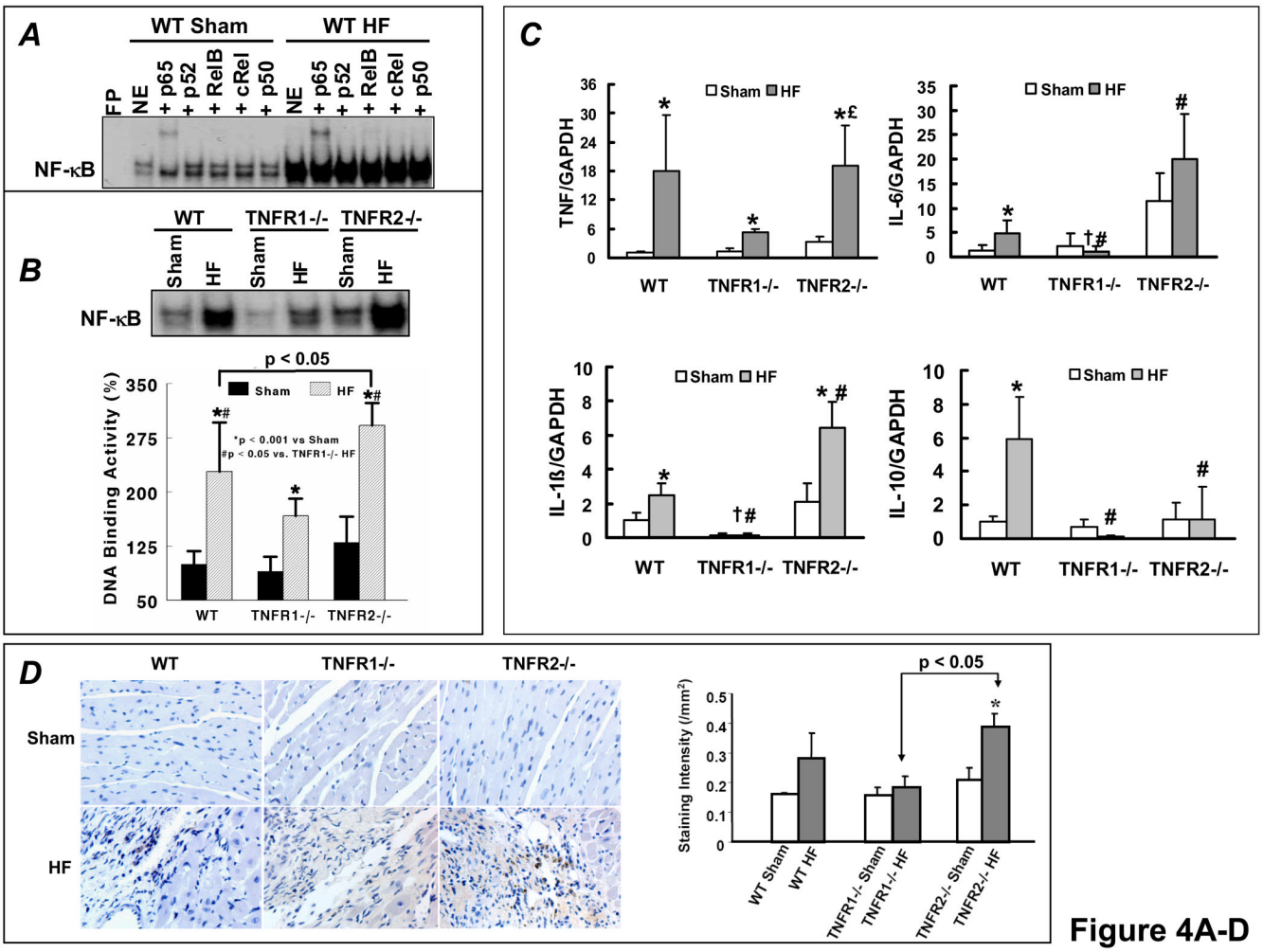

Figure 4A-D

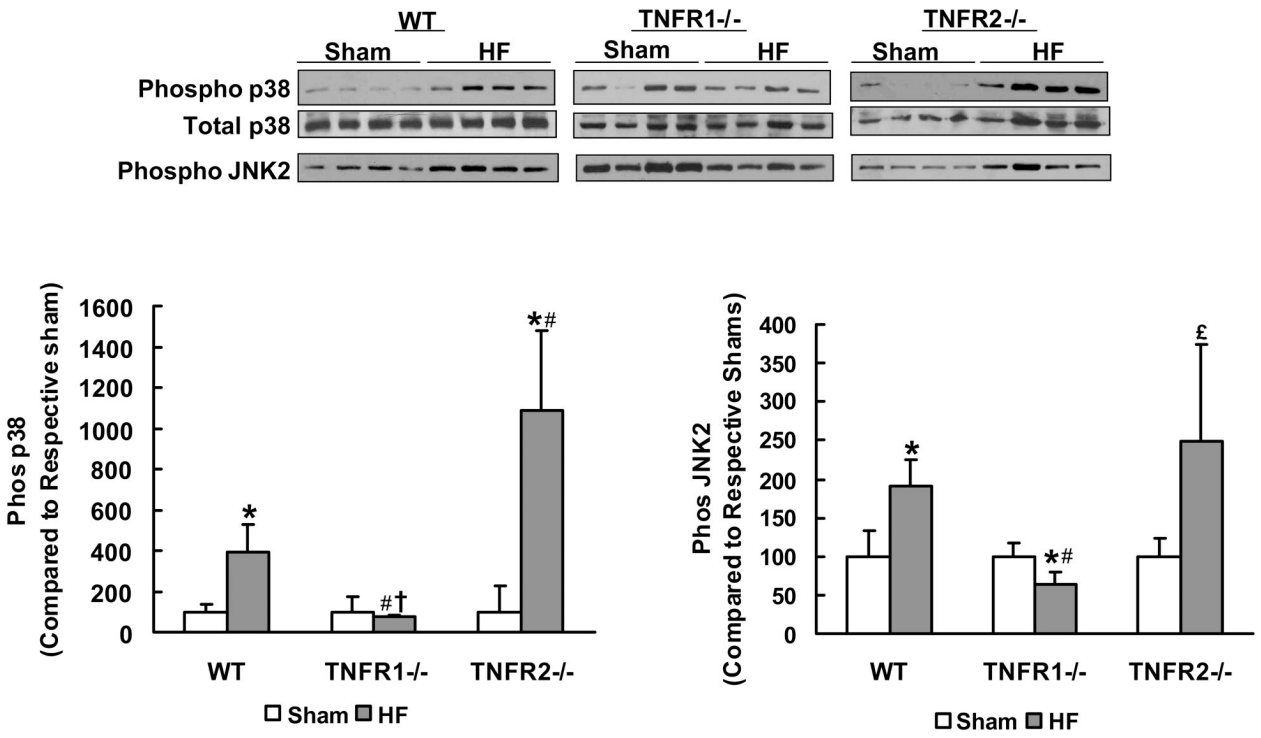

Figure 4E

Figure 4.

TNFR1 and TNFR2 induce divergent NF-κB and inflammatory signaling responses in HF. *(A)* NF-κB DNA binding activity and subunit composition by EMSA and gel supershifts in nuclear extracts from WT sham and HF hearts. *(B)* NF-κB DNA-binding activity in nuclear extracts from WT, TNFR1−/−, and TNFR2−/− sham and HF hearts. *(C)* Normalized gene expression of TNF, IL-1β, IL-6 and IL-10 by qRT-PCR analysis (n=6/group). *(D)* Anti-MOMA-2 immunohistochemistry for activated macrophages (brown staining) in sham and failing hearts and corresponding quantitation. *(E)* Western-blots and densitometry for phospho/total p38 and phospho-JNK2 in sham and failing LV tissue. *p<0.05 vs. sham, $^{\#}$p<0.05 vs. WT HF, †p<0.05 vs. TNFR2−/− HF, $^{£}$p<0.05 vs. TNFR1−/− HF.

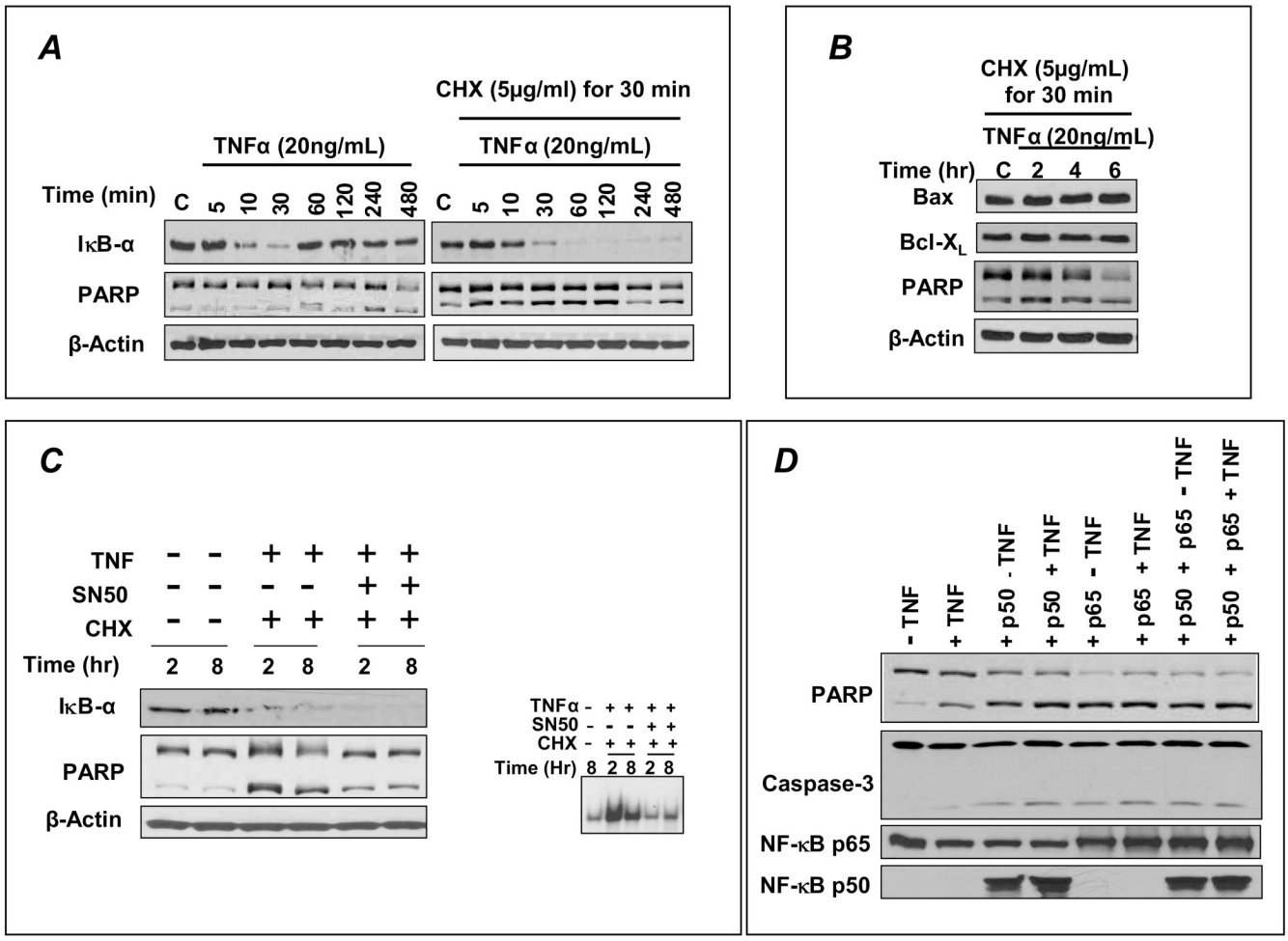

Figure 5A-D

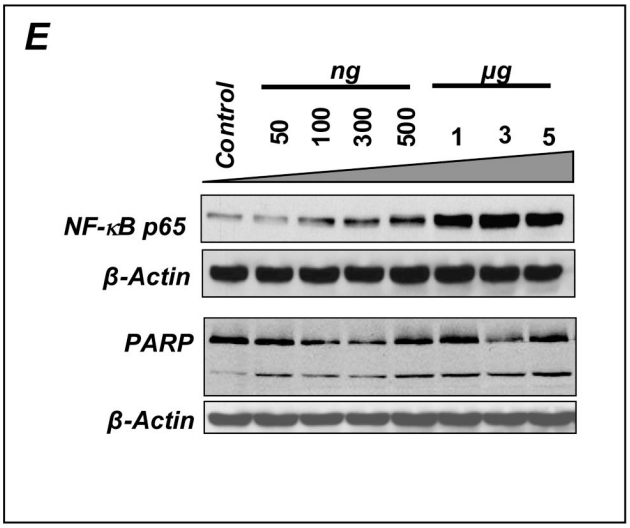

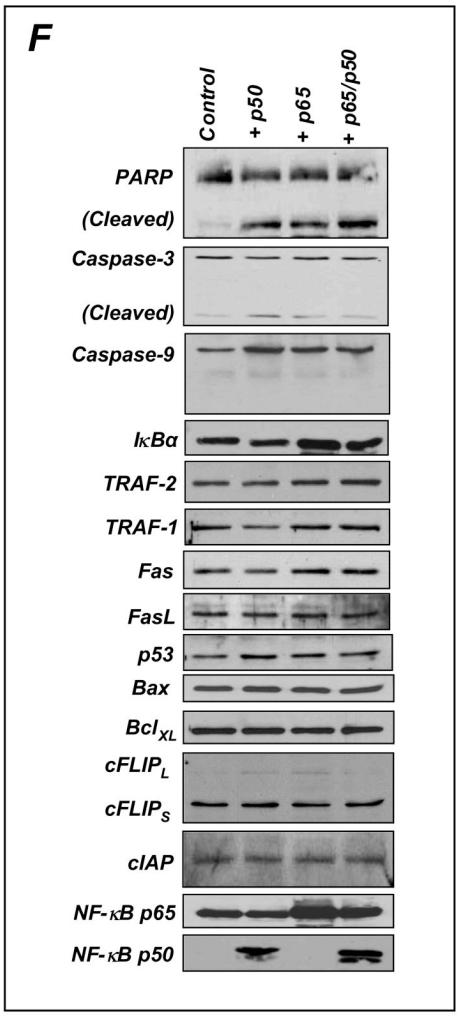

Figure 5E,F

Figure 5.

Sustained NF-κB activation is pro-apoptotic in H9c2 cardiomyocytes. *(A)* H9c2 cells were treated with TNF with or without pretreatment with the protein synthesis inhibitor cycloheximide (CHX) and cell lysates were analyzed by Western blotting. TNF induced rapid IκBα degradation with resynthesis within 1 h but no apoptosis as indicated by predominantly uncleaved PARP. CHX pretreatment prevented IκBα resynthesis and induced apoptosis (augmented cleaved PARP). *(B)* Bcl-X_L protein expression and the Bcl-X_L/Bax ratio with CHX pretreatment and TNF stimulation. *(C)* Pre-incubation with SN50, a peptide inhibitor of NF-κB nuclear translocation, attenuated apoptosis. *(D)* H9c2 cells were transfected with either empty vector (pcDNA 3.1) or p65 and/or p50 expression vectors for 24 h followed by treatment with or without TNF for 8 h. Sustained p65 or p50 overexpression augmented PARP and caspase-3 cleavage, irrespective of TNF exposure. *(E)* H9c2 cells were transfected for 24 h with increasing amounts of p65 expression vector and total amount of DNA was compensated with pcDNA3.1. The apoptotic effect of p65 exhibited dose-dependency. *(F)* H9c2 cells transfected with p65 and/or p50 for 24 h did not exhibit changes in expression of a variety of pro-and anti-apoptotic proteins including TRAF-1 and 2, Fas and FasL, Bax and Bcl-X_L, cFLIP and cIAP, and p53. Results in A–F are representative of four independent experiments.

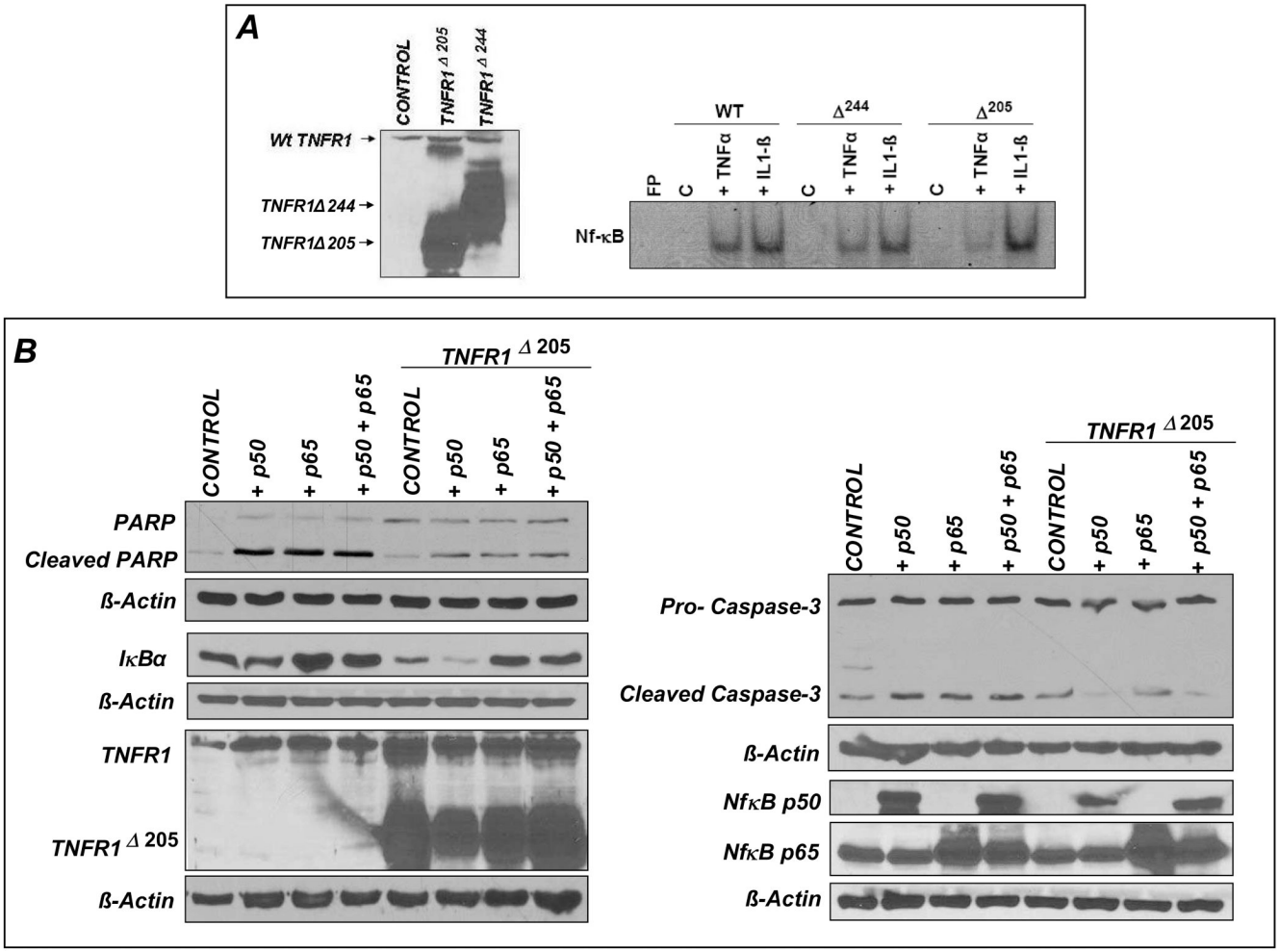

Figure 6A,B

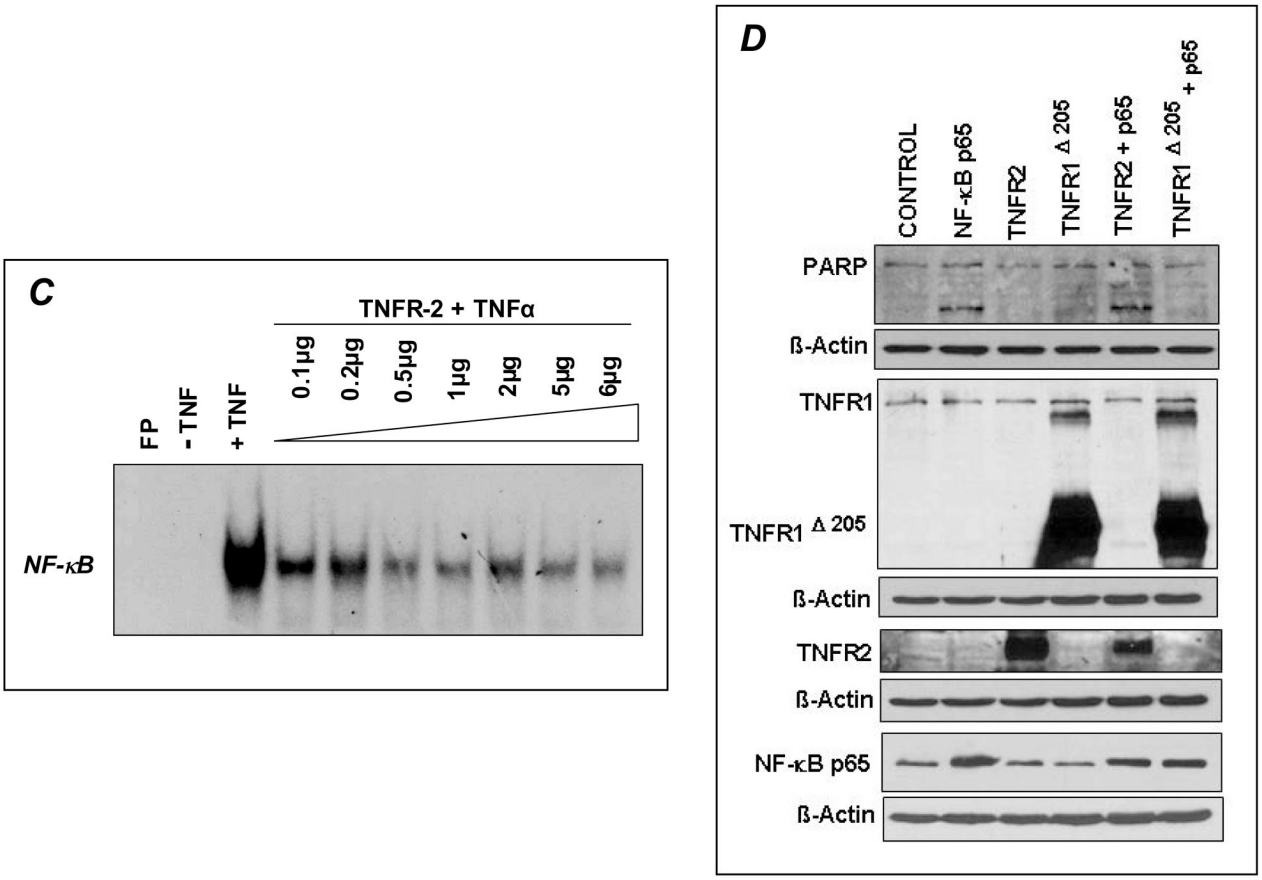

Figure 6C,D

Figure 6.

TNFR1 and TNFR2 uniquely modulate NF-κB activation. *(A)Left*, H9c2 cells were transfected (5µg) with either control vector (pcDNA3.1) or vectors encoding truncated human TNFR1 (TNFR1Δ244 or TNFR1Δ205) for 24 h and whole cell lysates were analyzed for TNFR1 expression by Western blotting. *Right*, similarly transfected cells were treated with either TNF or IL-1β for 30 min and NF-κB DNA-binding activity examined by EMSA. *(B)* H9c2 cells were (co-)transfected (6µg) for 24 h with p65 and/or p50 expression vectors and TNFR1Δ205. As indexed by PARP and caspase-3 cleavage, the pro-apoptotic effects of p65 and p50 were attenuated by TNFR1Δ205. *(C)* H9c2 cells were transfected with increasing quantities of full-length TNFR2 for 24 h followed by treatment with TNF for 30 min. Total amount of DNA (6µg) was compensated with pcDNA3.1. EMSA revealed that TNFR2 overexpression reduced TNF-induced NF-κB activation in a dose-dependent manner. *(D)* H9c2 cells were (co)-transfected (5µg) with vectors encoding p65 and/or TNFR2 for 24 h. p65 and TNFR2 co-transfection did not reduce PARP cleavage. Results in A–D are representative of three independent experiments.

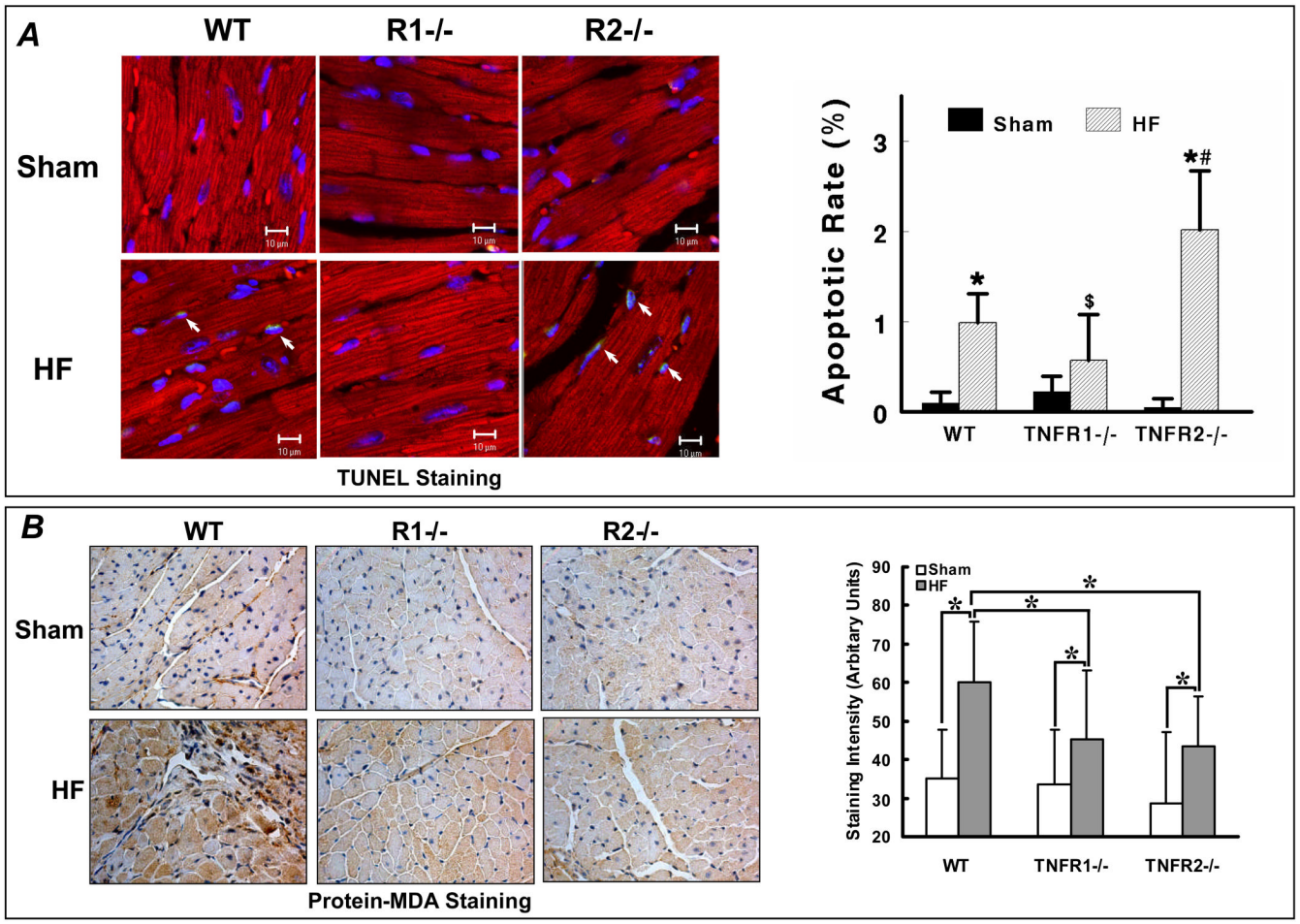

Figure 7.

TNFR1 and TNFR2 induce divergent effects on apoptosis but similar effects on oxidative stress in HF. *(A)* Apoptosis was quantified by APO-BrdU TUNEL Assay in WT, TNFR1−/−, and TNFR2−/− sham and HF hearts. Co-staining was performed with a-actinin (red) to identify myocytes and DAPI (blue) to identify nuclei. Apoptotic nuclei are cyan (arrows). *p<0.05 vs. sham, $^{\#}$p<0.05 vs. WT HF, $^{\$}$p<0.05 vs. TNFR2−/− HF. *(B)* Protein-MDA immunostaining (brown staining) as an index of oxidative stress from the same experimental groups. *p<0.05.

Table

LV Hemodynamics in WT, TNFR1−/−, and TNFR2−/− Sham and HF Mice

	WT		TNFR1−/−		TNFR2−/−	
	Sham (n = 15)	**HF (n = 21)**	**Sham (n = 7)**	**HF (n = 11)**	**Sham (n = 8)**	**HF (n = 15)**
HR	539 ± 50	431 ± 49*	519 ± 36	511 ± 47$^{\#}$	530 ± 35	475 ± 53$^{*\#}$
LVPSP	98 ± 8	86 ± 8*	99 ± 10	96 ± 8$^{\#}$	98 ± 12	84 ± 5$^{*\wedge}$
dP/dt_{max}	10245 ± 2054	4962 ± 1346*	9328 ± 2084	7167 ± 1426$^{*\#}$	9611 ± 1659	4997 ± 993$^{*\wedge}$
dP/dt_{max}/IP	185 ± 35	98 ± 22*	165 ± 29	118 ± 19$^{*\#}$	170 ± 34	101 ± 22$^{*\wedge}$
LVEDP	8 ± 3	16 ± 4*	7 ± 1	12 ± 4$^{*\#}$	9 ± 3$^{\$}$	8 ± 4$^{\#\wedge}$
Tau	9.1 ± 2.1	18.8 ± 3.6*	10.4 ± 2.9	14.0 ± 2.3$^{*\#}$	10.4 ± 1.8	15.2 ± 2.8$^{*\#}$

LV, left ventricular; HR, heart rate (bpm); LVPSP, LV peak systolic pressure (mm Hg); dP/dt_{max}, maximal rate of change in LV pressure (mm Hg/s); dP/dt_{max}/IP, dP/dt_{max} normalized fro instantaneous LV pressure (s^{-1}); LVEDP, LV end-diastolic pressure (mm Hg); tau, time constant of LV relaxation (ms); All values mean ± SD.

* $p < 0.05$ vs. respective sham,

$^{\$}$ $p < 0.05$ vs. TNFR1−/− sham,

$^{\#}$ $p < 0.05$ versus WT HF,

$^{\wedge}$ $p < 0.05$ vs. TNFR1−/− HF.